Pharm Res (2017) 34:2084–2096
DOI 10.1007/s11095-017-2213-4

RESEARCH PAPER

Anti-Tuberculosis Bacteriophage D29 Delivery with a Vibrating Mesh Nebulizer, Jet Nebulizer, and Soft Mist Inhaler

Nicholas B. Carrigy[1] • Rachel Y. Chang[2] • Sharon S. Y. Leung[2] • Melissa Harrison[3] • Zaritza Petrova[4] • Welkin H. Pope[4] • Graham F. Hatfull[4] • Warwick J. Britton[5] • Hak-Kim Chan[2] • Dominic Sauvageau[3] • Warren H. Finlay[1] • Reinhard Vehring[1,6]

Received: 27 March 2017 / Accepted: 14 June 2017 / Published online: 23 June 2017

ABSTRACT

Purpose To compare titer reduction and delivery rate of active anti-tuberculosis bacteriophage (phage) D29 with three inhalation devices.

Methods Phage D29 lysate was amplified to a titer of 11.8 ± 0.3 $\log_{10}$(pfu/mL) and diluted 1:100 in isotonic saline. Filters captured the aerosolized saline D29 preparation emitted from three types of inhalation devices: 1) vibrating mesh nebulizer; 2) jet nebulizer; 3) soft mist inhaler. Full-plate plaque assays, performed in triplicate at multiple dilution levels with the surrogate host *Mycobacterium smegmatis*, were used to quantify phage titer.

Results Respective titer reductions for the vibrating mesh nebulizer, jet nebulizer, and soft mist inhaler were 0.4 ± 0.1, 3.7 ± 0.1, and 0.6 ± 0.3 $\log_{10}$(pfu/mL). Active phage delivery rate was significantly greater ($p < 0.01$) for the vibrating mesh nebulizer ($3.3x10^8 \pm 0.8x10^8$ pfu/min) than for the jet nebulizer ($5.4x10^4 \pm 1.3x10^4$ pfu/min). The soft mist inhaler delivered $4.6x10^6 \pm 2.0x10^6$ pfu per 11.6 ± 1.6 μL ex-actuator dose.

Conclusions Delivering active phage requires a prudent choice of inhalation device. The jet nebulizer was not a good choice for aerosolizing phage D29 under the tested conditions, due to substantial titer reduction likely occurring during droplet production. The vibrating mesh nebulizer is recommended for animal inhalation studies requiring large amounts of D29 aerosol, whereas the soft mist inhaler may be useful for self-administration of D29 aerosol.

KEY WORDS aerosol · *Mycobacterium tuberculosis* · nebulization · phage therapy · titer reduction

ABBREVIATIONS

g	Gravitational acceleration
i	Nebulization cycle count
$\log_{10}$	Base 10 logarithm
MDR-TB	Multidrug-resistant tuberculosis
MOI	Multiplicity of infection
n	Number of plates
pfu	Plaque-forming unit
Phage	Bacteriophage
TB	Tuberculosis
TEM	Transmission electron micrograph
XDR-TB	Extensively drug-resistant tuberculosis

INTRODUCTION

Increasing incidence of bacterial resistance to antibiotics is a threat to global health [1]. For example, multidrug-resistant tuberculosis (MDR-TB), defined as resistant to the first-line antibiotics isoniazid and rifampicin, was observed in 3.3% of new TB cases globally in 2014 and 2015 [2]. Extensively drug-resistant TB (XDR-TB), which is resistant to the most effective second-line anti-TB antibiotics, occurred in 9.5% of MDR-TB cases [2]. Totally drug-resistant TB has also been reported [3], although it is classified as XDR-TB by the World Health

✉ Reinhard Vehring
reinhard.vehring@ualberta.ca

[1] Department of Mechanical Engineering, University of Alberta, Edmonton, AB, Canada

[2] Advanced Drug Delivery Group, Faculty of Pharmacy, University of Sydney, Sydney, Australia

[3] Department of Chemical and Materials Engineering, University of Alberta, Edmonton, AB, Canada

[4] Department of Biological Sciences, University of Pittsburgh, Pittsburgh, PA, USA

[5] Centenary Institute of Cancer Medicine and Cell Biology, and Sydney Medical School, University of Sydney, Sydney, Australia

[6] Department of Mechanical Engineering, 10-203 Donadeo Innovation Centre for Engineering, University of Alberta, 9211 116th Street NW, Edmonton, AB T6G 1H9, Canada

Organization [4]. Exacerbating antibiotic resistance is the slow commercialization of new antimicrobials [1].

Bacteriophage (phage) therapy may be useful as an alternative or adjunct to antibiotics [5–7]. Phage are bacterial viruses that typically infect a narrow-spectrum of bacteria within a single genus [8, 9], thus only minimally harming flora during phage therapy [9]. Additionally, antibiotic-resistance does not translate into phage-resistance [9]. Phage also have low inherent toxicity, and in some cases, have the potential to cause biofilm degradation [9].

Phage have co-evolved with bacteria and are the most numerous biologic entities on Earth [10]. New phage strains able to infect new pathogenic bacteria can be found relatively rapidly [9]. While not all phage are useful for therapeutic purposes, stable, lytic phage that effectively kill their host bacteria are routinely selected with the aid of genome sequencing and analysis [8]. A lytic phage binds to its target bacterium and injects its genetic material through the cell wall, initiating the biosynthesis of new phage within the bacterium [10]. These progeny phage, which can be produced on the order of one hundred per bacterium [11], escape by lysing the cell wall (which kills the bacterium) and go on to infect and replicate within neighbouring bacteria until all accessible and susceptible host bacteria are lysed [10].

Respiratory delivery of phage is an active topic in research and development [11, 12], with phage-containing dosage forms for nebulizers and dry powder inhalers, and even some exploratory versions for pressurized metered dose inhalers, tested *in vitro* [13–17]. Phage are generally regarded as safe, exhibiting few if any side effects [12]. In Georgia and Russia, oral phage cocktails are even available to the public without prescription [5]. However, the development of commercial phage products for human therapy in Western medicine has been hindered by a relative lack of private investment due in part to uncertainty over timelines necessary for obtaining regulatory approval [18, 19].

Humans have been treated clinically using pulmonary phage delivery in parts of Eastern Europe, with efficacy reports being generally positive [5, 20]. Excellent reviews of aerosol phage therapy have also been published [8, 11, 20]. However, human pulmonary delivery studies coming out of Eastern Europe do not conform to the standards required by regulatory authorities in the United States. Before more comprehensive studies in humans can be performed, animal studies to demonstrate safety and efficacy are a logical first step. To this end, Semler *et al.* [21] recently delivered phage from the family *Myoviridae* to mice using a nose-only inhalation device to treat antibiotic-resistant lung infections. This study showed that efficacy of phage delivered by inhalation was superior to that of phage delivered to control mice intraperitoneally, with a greater decrease in bacterial count and evidence of phage replication in the lungs [21]. In the Semler *et al.* [21] study, the success of phage therapy relied upon the delivery of enough active phage to start infection of the bacteria. The ratio of active phage to target bacteria is termed multiplicity of infection (MOI) and was a critical formulation design factor.

To ensure a high MOI in pulmonary phage delivery, titer reduction due to aerosolization should be minimized. Ensuring minimal titer reduction also decreases production costs and the chances of negative side effects associated with formulation excipients. For delivery to the lungs, undesirable titer reductions in the systemic system are circumvented when inhaled aerosol delivery is used instead of injection. Indeed, Liu *et al.* [22] found a higher concentration of active phage D29 in the lungs using inhaled aerosol delivery than using injection. However, stresses acting on phage in some inhalation devices can cause substantial titer reduction. A further discussion of factors that can contribute to phage titer reduction is given elsewhere [10, 11]; these include temperature, shear, and osmotic shock.

This study examines how effectively a vibrating mesh nebulizer, a jet nebulizer, and a soft mist inhaler deliver active phage. To the authors' knowledge, the soft mist inhaler, which has the advantages of portability and electricity-free operation, has never before been tested with phage. Nebulizers, unlike metered-dose inhalers and dry powder inhalers, have the advantage of being able to deliver filtered phage lysate without further processing. Moreover, nebulizers can deliver large amounts of aerosol continuously, including to those unable to coordinate the breathing maneuver required for inhalers, and can be more easily coupled to animal exposure devices. Nebulizers can also deliver resuspended phage powder should the need arise. Jet nebulizers and vibrating mesh nebulizers have previously been tested with phage [14, 23, 24]; however, as far as the authors are aware, titer reduction and active phage delivery rate with these devices has never before been directly tested with phage D29. This lytic phage (Fig. 1) is of particular interest as it can effectively kill a range of mycobacteria, including *Mycobacterium tuberculosis* [25]. Indeed, phage D29 is commonly used for TB diagnosis and drug-susceptibility testing [8]. It is of the *Caudovirales* order,

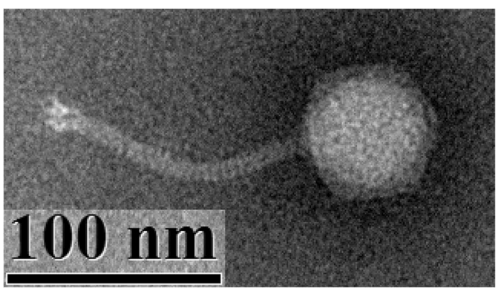

Fig. 1 Transmission electron micrograph (TEM) (80 kV operation, Model: Morgagni 268; Philips – FEI, Hillsboro, Oregon, USA; with Gatan Orius CCD Camera and Gatan DigitalMicrograph™ Software Version 1.81.78) of phage D29. To generate the sample for imaging, a drop of lysate was placed on a TEM grid (300 mesh Copper grids with Formvar/Carbon Support Film; Prod # 01753-F; Ted Pella Inc., Redding, CA, USA), stained with 2% phosphotungstic acid for 30 s, and then removed using filter paper.

having an icosahedral capsid (~55 nm 'wide') containing double-stranded deoxyribonucleic acid and a tail [8]. Its characteristic of a long (~130 nm), flexible and non-contractile tail places it in the *Siphoviridae* morphological family [8].

MATERIALS AND METHODS

Phage D29 Bioprocessing and Shipping

High titer phage D29 lysate was generated and titered using well-established protocols [26]. Briefly, D29 from a laboratory stock was amplified on the host *Mycobacterium smegmatis* strain mc^2155 using solid media. A plate with confluent plaques was flooded with phage buffer, incubated overnight at 4°C, harvested and filtered through a 0.22 μm filter. The lysate was further concentrated by centrifugation at $2.06x10^5$ m/s^2 [21,000 x g] for 90 min at 4°C, and pellet resuspension in phage buffer (10 mM $MgSO_4$, 1 mM $CaCl_2$, 10 mM Tris(hydroxymethul)aminomethane 7.5, and 68.5 mM NaCl). After amplification, ~2 mL of lysate was shipped from the University of Alberta, Canada, to the University of Sydney, Australia to perform the experiments. The phage lysate was wrapped in cold packs in an insulated Styrofoam container and sent using 2-day express shipping. The temperature during shipment was monitored and recorded (TempTale 4 USB MultiAlarm; Sensitech Canada; Markham, ON, Canada) and found to increase from 5°C to 20°C within the Styrofoam container over the two-day period, with a mean temperature of 11°C. No titer reduction was observed under these shipping conditions. Separate measurements of crude D29 lysate indicated no titer reduction after six weeks and ~2 $\log_{10}$(pfu/mL) titer reduction after 10 months of storage at 4°C.

Plaque Assay Method

Plaque assays used the surrogate *M. smegmatis* mc^2155. The full-plate titer method, detailed elsewhere [26], was used, as the plaques were too large for spot assay. The plaque assays were performed in triplicate at multiple dilution levels. Negative control measurements were performed to confirm the absence of phage contamination in the stock materials.

Dilution Stability Test Method

The amplified phage lysate was diluted 1:100 in isotonic saline (9 mg/mL sodium chloride (Sigma S5886, Lot#078K01272; Sigma Aldrich; St. Louis, MO, USA) in MilliQ water) within a 15 mL Falcon tube, and plaque assays were performed at time points of 0, 1.5, and 18 h to compare the titer prior to and after dilution. This dilution lowers the concentration of components in the lysate that may not be suitable for inhalation at high concentrations, such as Tris pH 7.5. An additional diluted lysate sample was micropipetted onto a filter and left at room temperature for 50 min to verify whether some titer reduction could be due to phage binding to the filter during an experiment. All measurements were made at room temperature.

Aerosolization Titer Reduction Test Method

The three clinically-relevant inhalation devices tested were 1) Aerogen Solo vibrating mesh nebulizer (Model No. 06675745, Lot 60201509300103, Ref AG-AS3350-US; Aerogen Ltd., Dangan, Galway, Ireland) with Pro-X Controller (S/N AP-1510412, Ref AG-PX-1050-IN; Aerogen Ltd., Dangan, Galway, Ireland); 2) Pari LC Sprint jet nebulizer (Part # 023F35-C; Pari Respiratory Equipment, Inc.; Midlothian, VA, USA) with Pari Boy SX Compressor (S/N: 2W14J03112; Type 085; Pari GmbH, Starnberg, Germany); 3) Respimat soft mist inhaler (Lot 401445B; Boehringer Ingelheim (Canada) Ltd., Burlington, ON, Canada).

For each run, a known volume from the stock of amplified phage lysate was diluted 1:100 in isotonic saline to create a saline phage D29 preparation, which was then pipetted into the inhalation device reservoir. Fill volumes were 6 mL for the vibrating mesh nebulizer, 8 mL for the jet nebulizer, and 4 mL for the soft mist inhaler. A filter (Suregard Bacterial/Viral Respiratory Filter; BIRD Healthcare, Port Melbourne, VIC, Australia) was connected to the aerosol outlet of the tested device. The aerosolized droplets were captured on the filter, without the use of breathing simulation.

For the vibrating mesh nebulizer, enough liquid was collected on the filter that it could be drawn directly for plaque assay to determine the output titer. The recovered liquid from the filter was vortexed to ensure uniformity prior to assay.

For the soft mist inhaler, a custom adapter made with a PolyJet 3D printer (Objet Eden 350 V High Resolution 3D Printer; Stratsys, Ltd.; Eden Prairie, MN, USA) from an acrylic compound (Objet VeroGray RGD850; Stratsys, Ltd.; Eden Prairie, MN, USA) connected the filter to the mouthpiece. The small dose of liquid emitted from the soft mist inhaler meant that 10 actuations onto the filter and resuspension in phage buffer were necessary to draw liquid for plaque assay. The ex-actuator dose from the soft mist inhaler was measured by weighing the inhaler with a microbalance before and after 10 actuations. The dilution ratio occurring from phage buffer resuspension was determined using the gravimetrically measured ex-actuator dose of 11.6 ± 1.6 μL per actuation, which is within error of the expected 11.05 μL per actuation [27], and the known volume (10 mL) of phage buffer added to the filter in increments of 1 mL with a micropipette. The extra dilution was accounted for in output titer calculation. Additionally, the drug solution is normally stored in a cartridge that consists of an aluminium cylinder containing a double-walled polypropylene collapsible bag which contracts

as the solution is withdrawn [28, 29]; in the present study, the polypropylene bag was used without the aluminium cylinder to allow for refilling of the phage solution.

Experiments with a titer reduction detection limit of ~3 $\log_{10}$(pfu/mL) for the jet nebulizer produced no plates with ≥5 plaques. Further measurements with the jet nebulizer utilizing a titer reduction detection limit of ~4 $\log_{10}$(pfu/mL) were performed with aerosol collected on separate filters after 7 min, the subsequent 11 min, and the subsequent 24 min of nebulization. For these experiments, dilution of the liquid recovered on the filter was also performed with 10 mL of phage buffer. The filter mass was measured with a microbalance before and after nebulization to determine the dilution ratio and delivered volume.

Titer reduction was quantified as the difference in the base 10 logarithm of plaque-forming units per millilitre ($\log_{10}$(pfu/mL)) between the saline phage preparation input to the inhalation device and the aerosol collected on the filter after exiting the inhalation device. Percent deactivation due to aerosolization was calculated as [1 – (output titer per millilitre collected on the filter / input titer per millilitre of saline phage preparation input to the inhalation device)] * 100%.

Nebulization Cycle Count Method

For the jet nebulizer, only a fraction of the liquid exiting the nozzle in the form of primary droplets continues on to exit the mouthpiece, since much of the liquid from the droplets impacting the baffles and inner walls of the device return to the reservoir for renebulization. To quantify this fraction, the flow rates of liquid forming primary droplets and exiting the mouthpiece were determined separately as shown in Fig. 2. The measurement of the flow rate exiting the nozzle was determined using Tryptophan (L-Tryptophan; Cat #93659; Sigma Aldrich; St. Louis, MO, USA) in isotonic saline as a tracer, with the collecting filter assayed using UV spectrophotometry (8452A Diode Array Spectrophotometer; Hewlett-Packard, Mississauga, ON, Canada). The ambient air temperature and humidity for these measurements were approximately 23°C and 20% relative humidity. A mathematical model, given in the Appendix, was developed to determine the average number of nebulization cycles undergone by the phage, i.e. the average number of times phage exited the nozzle and impacted the primary baffle prior to exiting the mouthpiece of the jet nebulizer. This impaction count may be an indicator of the cumulative stress the phage encounter before exiting the mouthpiece.

Titer Delivery Rate Method

The number of active phage delivered per minute is of interest for inhalation studies with nebulizers, since long exposure times may not be practical and phage clearance may be relatively quick. Time-averaged aerosol production rate was determined for the vibrating mesh nebulizer using the time required to deplete the entire fill volume, as the residual volume was negligible. For the jet nebulizer, humidification of the air supplied by the compressor results in loss of solvent mass, and the residual volume was 0.5 mL; thus, the aerosol production rate was determined using both the mass captured on a filter during aerosolization titer reduction experiments and the time over which the nebulization occurred. The active phage delivery rate for each nebulizer was calculated using the output titer and the measured aerosol production rates.

For the soft mist inhaler, the number of active phage delivered per actuation is a more relevant delivery parameter than the number of active phage delivered per minute. The number of active phage delivered per actuation from the soft mist

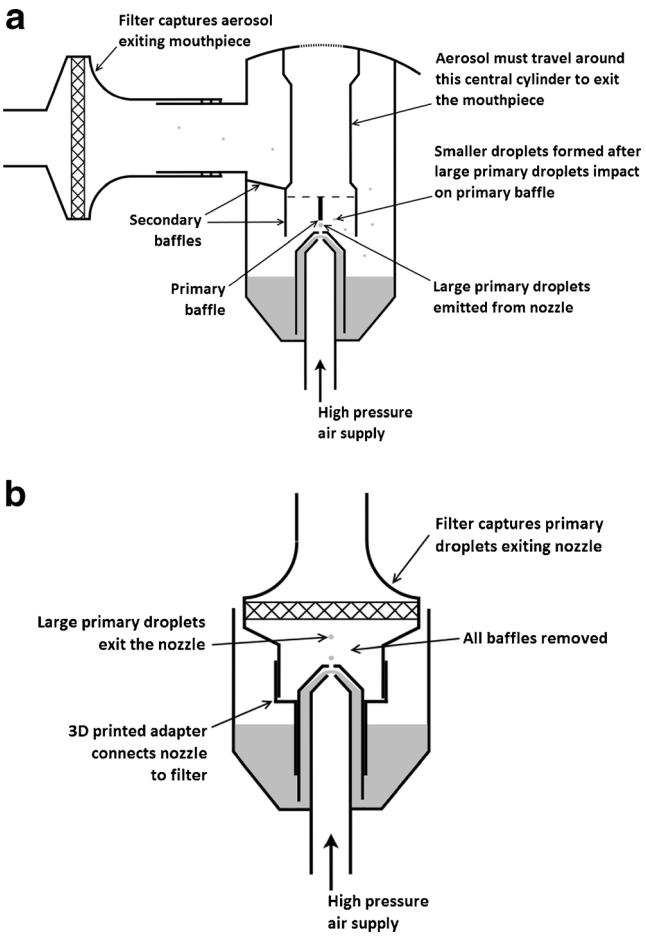

Fig. 2 Schematic of filter measurements used to determine the flow rate of droplets exiting (**a**) the mouthpiece, using the unmodified jet nebulizer and (**b**) the nozzle in the form of primary droplets, using a jet nebulizer with all baffles removed. A fraction of the liquid volume from the droplets which impact the baffles and inner walls of the device in (**a**) is returned to the reservoir for renebulization. The experimental results for flow rate in each case were used as input to the mathematical model given in the Appendix to predict the number of nebulizations phage underwent prior to exiting the mouthpiece. Figures not to scale.

inhaler was calculated using the gravimetrically measured emitted dose of aerosol and the measured output titer.

Statistical Method

Results are presented as mean ± standard deviation using results where plates had ≥5 plaques per plate. The number of plates used to calculate mean and standard deviation ranged from 2–8. Statistical comparisons utilized the Student's t-test without assuming equal variance, at a significance level of 0.05.

RESULTS

Dilution Stability

The stability of phage D29 diluted in isotonic saline was measured (Table I) for well over the maximum expected timeframe of an aerosolization experiment (50 min) to determine whether the dilution step would cause unexpected titer reduction during experimentation. Titer immediately after 1:100 dilution was 9.9 ± 0.1 $\log_{10}$(pfu/mL), which was not significantly different ($p > 0.1$) from the expected 9.8 ± 0.3 $\log_{10}$(pfu/mL), indicating the dilution itself did not lead to unexpected titer reduction in a Falcon tube. Furthermore, the titer of the saline phage preparation was not significantly different from the expected value ($p > 0.1$) after 18 h at room temperature. There was also no indication of phage binding to the filter ($p > 0.1$). These results indicated that the test method itself was not a cause of significant titer reduction.

Plaque assays on the diluted saline phage preparation kept in a Falcon tube were also performed after each aerosolization experiment (termed input titer). In each case, an input titer >9 $\log_{10}$(pfu/mL) was observed, further verifying the stability of D29 after dilution in isotonic saline at room temperature.

Table I Stability of phage D29 lysate at various time points after 1:100 dilution in isotonic saline in a 15 mL Falcon tube, and after dilution and 50 min storage in a filter. All measurements were at room temperature. For no time point was titer after dilution significantly different from the expected 9.8 ± 0.3 $\log_{10}$(pfu/mL) ($p > 0.1$)

Test	Time [min]	Titer [($\log_{10}$(pfu/mL)]
Pre-Dilution	-	11.8 ± 0.3
1:100 Dilution - Tube	0	9.9 ± 0.1
	90	10.0 ± 0.4
	1080	9.6 ± 0.2
1:100 Dilution - Filter	50	9.4 ± 0.6

Aerosolization Titer Reduction

The input titers for the vibrating mesh nebulizer, jet nebulizer, and soft mist inhaler were respectively $2.3x10^9 \pm 0.4x10^9$, $2.4x10^9 \pm 0.3x10^9$, and $1.4x10^9 \pm 0.5x10^9$ pfu/mL, which were not significantly different from each other ($p > 0.1$). The respective output titers were $9.0x10^8 \pm 2.0x10^8$, $4.4x10^5 \pm 1.1x10^5$, and $4.0x10^8 \pm 1.6x10^8$ pfu/mL. The percent deactivation due to aerosolization was thus 60 ± 11%, 99.981 ± 0.005%, and 72 ± 14% for the respective inhalation devices. Figure 3 illustrates the titer reduction, calculated as the $\log_{10}$ of input titer per mL minus the $\log_{10}$ of output titer per mL, for each inhalation device.

Titer reduction due to aerosolization was ~0.5 $\log_{10}$(pfu/mL) for both the vibrating mesh nebulizer and the soft mist inhaler. There was no significant difference in titer reduction between these two devices ($p > 0.1$). Titer reduction was significantly greater for the jet nebulizer than for either the soft mist inhaler or the vibrating mesh nebulizer ($p < 0.0005$).

Nebulization Cycle Count

The jet nebulizer is designed so that droplets which impact and spread on the baffles and nebulizer walls, being unable to return to the airflow, are returned (drip back) to the reservoir for renebulization [30]. The flow rate of droplets exiting the mouthpiece of the jet nebulizer was 0.122 ± 0.003 mL/min, while the flow rate of primary droplets exiting the nozzle was 17.6 ± 8.1 mL/min. These values were used in the mathematical model provided in the Appendix to calculate the cumulative percentage of phage (both active and inactive) that exited the mouthpiece of the jet nebulizer after each nebulization cycle, relative to the initial number of phage in the reservoir. The result is given in Fig. 4, along with the average number of times phage (regardless of being active or inactive) were nebulized, i.e. exited the nozzle and impacted the primary baffle, prior to exiting the mouthpiece of the jet nebulizer. The results indicate that phage were exposed to the

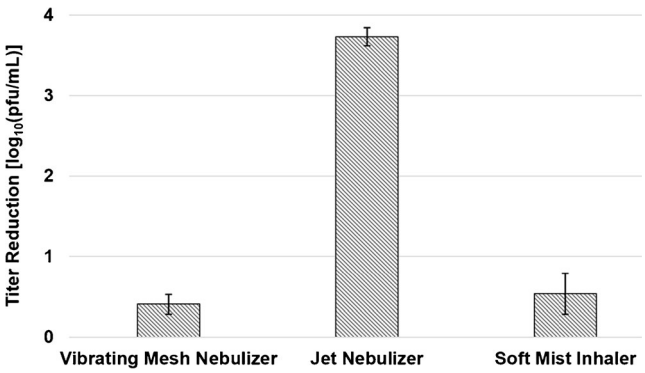

Fig. 3 Titer reduction of phage D29 due to aerosolization with each inhalation device.

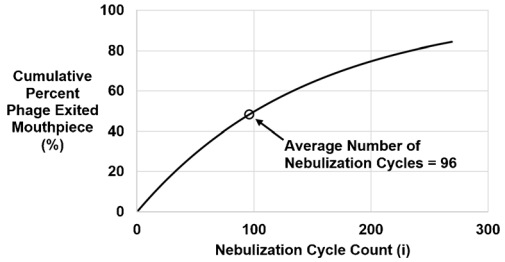

Fig. 4 Cumulative percent of initial number of phage in the reservoir that has exited the mouthpiece of the jet nebulizer, regardless of being active or inactive, for each nebulization cycle count, which is noted as i in the Appendix. Due to the residual volume, not all phage exited the mouthpiece. The average number of nebulization cycles the phage which exited the mouthpiece underwent is also indicated.

stresses of liquid breakup with a high-speed nozzle and impaction on the primary baffle an average of 96 times before exiting the mouthpiece. The predicted maximum number of nebulizations was 269, for the last phage exiting the mouthpiece and those remaining in the residual volume.

Active Phage Delivery Rate

Table II indicates the aerosol production rate and the number of active phage delivered per minute by the vibrating mesh nebulizer and by the jet nebulizer, as well as the number of active phage delivered per actuation by the soft mist inhaler.

Calculation shows the vibrating mesh nebulizer delivered active phage D29 ~ 6000 times faster than the jet nebulizer, which was statistically significant ($p < 0.01$). The more rapid active phage delivery rate is due mainly to the large titer reduction associated with the jet nebulizer, rather than to the difference in aerosol production rate. Calculation also shows that a single 11.6 μL ex-actuator dose from the soft mist inhaler, which lasts approximately 1.2 s [29], could deliver about as many active phage D29 as 1.5 h of delivery with the jet nebulizer, which would require about 15 mL of the same formulation.

DISCUSSION

Less than 1 $\log_{10}$(pfu/mL) titer reduction has been regarded in the literature as acceptable for nebulizing phage [11]. By this criterion, saline phage D29 preparation had an acceptable titer reduction when aerosolized with the vibrating mesh nebulizer, which uses the droplet production mechanism shown in Fig. 5. Briefly, this device operates by the converse piezoelectric effect, wherein an applied voltage causes a fluctuating change in volume of a piezoceramic ring element. This element is connected via a metal washer to a 5 mm diameter aperture plate, perforated with 1000 precision-formed holes, vibrating it at ~128 kHz [31]. The vibration consists of ~1 μm vertical displacement of the aperture plate, which extrudes formulation through the ~3 μm orifices in a micropump action [31] in what was found to be a relatively gentle process for phage D29. The quick delivery of large numbers of active phage with this device may make it particularly useful for animal studies as a high MOI may be achievable; additionally, it can be adapted to operate continuously with a syringe pump to potentially allow for hours of treatment with a high active phage delivery rate. Further methods to decrease titer reduction due to aerosolization using surfactants or other excipients have been proposed [13]; however, these excipients can complicate toxicology testing.

Saline phage D29 preparation also had acceptable titer reduction when aerosolized with the soft mist inhaler. Relevant components of this device are shown in Fig. 6. Briefly, when the base of this device is turned 180 degrees, a helical cam gear compresses a spring and lowers the capillary tube (which contains a one-way valve allowing liquid to travel only towards the nozzle) relative to the dosing chamber [29], drawing a pre-defined amount of liquid into the dosing chamber. When the dose-release button is pressed the spring releases, causing the capillary tube and one-way valve to move towards the nozzle outlet, thereby developing enough pressure downstream of the one-way valve to force the liquid through the pre-filter structure and nozzle outlet, where it collides in two small jets at an optimized angle to form a slowly moving aerosol [29]. The stresses acting on the phage in this device include pressure and shear. Hoe *et al.* [13] observed less than 1 $\log_{10}$ titer reduction after actuation of phage using a pressurized metered-dose inhaler, indicating their phage could survive relatively high levels of pressure and shear stress. This is in accord with the present study, where pressure and shear during soft mist inhaler actuation were relatively

Table II Aerosol production rate and active phage delivery rate for each inhalation device. The loaded dose was $1.36\times10^{10} \pm 0.21\times10^{10}$ pfu for the vibrating mesh nebulizer and $1.89\times10^{10} \pm 0.25\times10^{10}$ pfu for the jet nebulizer. Delivered dose was $5.40\times10^{9} \pm 1.20\times10^{9}$ pfu for the vibrating mesh nebulizer and $2.21\times10^{6} \pm 0.55\times10^{6}$ pfu for the jet nebulizer. Delivered dose as a percent of loaded dose was 39.7 ± 10.8% for the vibrating mesh nebulizer and 0.0117 ± 0.0033% for the jet nebulizer. Nebulization times were 17 min for the vibrating mesh nebulizer and 42 min for the jet nebulizer

Inhalation Device Type	Aerosol Production Rate	Active Phage Delivery Rate
Vibrating mesh nebulizer	0.364 ± 0.025 mL/min	$3.3\times10^{8} \pm 0.8\times10^{8}$ pfu/min
Jet nebulizer	0.122 ± 0.003 mL/min	$5.4\times10^{4} \pm 1.3\times10^{4}$ pfu/min
Soft mist inhaler	11.6 ± 1.6 μL/actuation	$4.6\times10^{6} \pm 2.0\times10^{6}$ pfu/actuation

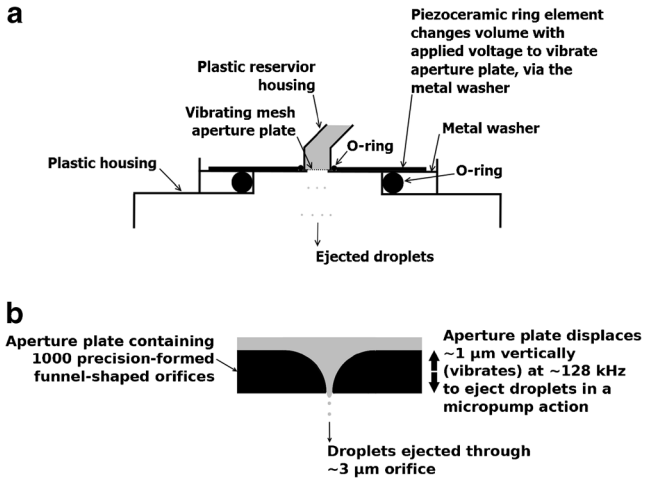

Fig. 5 Vibrating mesh nebulizer droplet production mechanism: (**a**) the structure surrounding the aperture plate (**b**) close-up of a funnel-shaped orifice in the aperture plate illustrating the micropump action, which ejects droplets. This droplet production mechanism was found to be relatively undamaging to phage D29. Figures not to scale.

unharmful to phage D29. Were the soft mist inhaler used without dilution, two orders of magnitude more active phage could potentially be delivered per actuation (~5 x 10^8 pfu per actuation). In addition, this device is compact and lightweight, features that may make it an attractive option for self-administration of phage aerosol.

In contrast to the other two inhalation devices, an unacceptably large titer reduction of ~3.7 $\log_{10}$(pfu/mL) occurred with the jet nebulizer. The mechanics of this device are described by Finlay [30]; see Fig. 2(a) for a diagram. Briefly, a pressurized air supply flows over a short section of liquid drawn up through a liquid feed tube by the low pressure at the orifice, through which gas accelerates. Downstream of the orifice the air jet travels at a higher relative velocity than the forming sheath of liquid formulation, which is subjected to the nonlinear development of unstable waves caused by the discontinuity of viscosity at the air-liquid interface. Primary droplets are produced by disintegration of the liquid sheath at the resonant wave crests, or other mechanisms. These larger primary droplets, which exit the nozzle, are then thought to break up into smaller droplets through impaction on the primary baffle, rather than through aerodynamic forces. These smaller droplets attain a velocity away from the primary baffle and head towards the mouthpiece. Some droplets further impact on secondary baffles or nebulizer walls and are returned to the reservoir for renebulization. Calculations using the results of tracer assay measurement show that in each cycle approximately 99% of the aerosol was renebulized, with an equivalent of the entire 8 mL fill volume being recirculated approximately every 30 s. These values agree with literature for the Collison triple-head jet nebulizer, for which 99.92% of aerosol exiting the nozzle was renebulized, with an equivalent of the entire 20 mL fill volume being recirculated every 6 s [32].

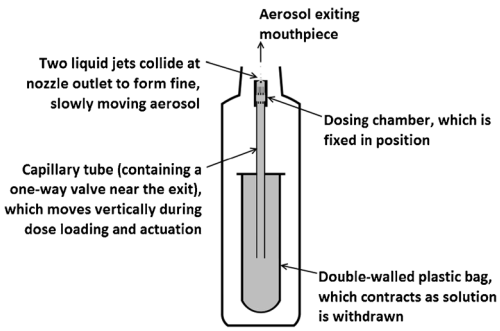

Fig. 6 Schematic of the soft mist inhaler. Shear and pressurization can occur throughout the device but these were relatively undamaging to phage D29. Figure not to scale.

In the present study, the first 10.5% of phage D29 in the reservoir that exited the mouthpiece of the jet nebulizer had undergone only 1–17 nebulization cycles but already had greater than 3 $\log_{10}$(pfu/mL) titer reduction. Thus, even relatively few nebulizations were damaging to most phage D29 within the preparation. It was suspected that large hydrodynamic stresses occurring during the baffle impaction primary droplet breakup process were responsible for the deactivation of liposomes and large molecules undergoing jet nebulization [30, 33]. These stresses could also be the cause of phage titer reduction in this study. A low recovery rate has also been noted by Liu *et al.* [34] for D29 delivered with a Collison jet nebulizer.

Comparing the titer reduction resulting from aerosolization in this study and in the literature indicates that it is device-dependent and phage strain-dependent. For example, Golshahi *et al.* [14] observed that *Myoviridae* phage KS4-M readily survived aerosolization with a jet nebulizer (Pari LC Star) and a vibrating mesh nebulizer (Pari eFlow), while Sahota *et al.* [24] found recovery of relatively fewer viable phage on an impactor for *Myoviridae* phage PELP20 using the Omron vibrating mesh nebulizer (~2 $\log_{10}$(pfu) reduction) than they did using the AeroEclipse jet nebulizer (~1 $\log_{10}$(pfu) reduction). These findings contrast with the present results, where the vibrating mesh nebulizer was less harmful to *Siphoviridae* phage D29 than the jet nebulizer. Sahota *et al.* [24] also noted lower titer recovery for *Myoviridae* phage PELI40 than for phage PELP20 with the jet nebulizer. Thus, given the present limited amount of data available in the literature, experimentally testing specific phage strains with specific inhalation devices is still necessary to determine the titer reduction due to aerosolization that will result, with ad-hoc predictions not advisable for new phage strains.

One direction that can be taken is to predict stress levels within prospective inhalation devices using a combination of experimental work, analytical modelling, and computational fluid dynamics [35]. The expected titer reduction could then be estimated from a titer reduction – stress level relationship

generated from experiments designed to measure titer reduction after exposure of phage to controlled stress levels. The devices could then be redesigned to minimize the stresses causing deactivation. However, testing different types of inhalation devices with a specific phage strain intended for a cocktail is still desirable in the development of inhalation device – phage cocktail combinations. Phage strains that may be useful in the development of an anti-TB phage cocktail are discussed elsewhere [8].

The respirable active phage delivery rate for the present inhalation devices can be calculated as the product of fine particle fraction, active phage delivery rate, and, for the nebulizers, the fraction of a breathing cycle spent inhaling. Using a fine particle fraction of 56% for the vibrating mesh and jet nebulizers [36, 37] and 69% for the soft mist inhaler [38], the active phage delivery rates given in Table II, and a fraction of the breathing cycle spent inhaling relevant for an adult male, 43.5% [30], the respirable active phage delivery rate was calculated to be $8.0x10^7$ pfu/min for the vibrating mesh nebulizer, $1.3x10^4$ pfu/min for the jet nebulizer, and $3.2x10^6$ pfu/actuation for the soft mist inhaler. The total respirable dose of active phage was $1.3x10^9$ pfu for the vibrating mesh nebulizer and $5.4x10^5$ pfu for the jet nebulizer. Some additional losses of phage due to extrathoracic deposition of fine particles can be expected to occur [30, 39].

The respirable dose of phage required to treat TB infection is not yet established. While Semler *et al.* [21] noted that successful treatment of antibiotic-resistant *Burkholderia cepacia complex* in mice required an MOI greater than 10 for treatment success, this bacteria group behaves differently in the lungs than TB, and therefore this MOI value is not expected to be directly relevant to D29. After entering the alveoli, TB bacteria are quickly engulfed by macrophages into phagosomes, where they may slow phagolysosome formation and survive the acidic phagolysosome compartments which do form [40]. Xiong *et al.* [41] showed that the titer of D29 is higher after uptake in TB-infected macrophages than after uptake in uninfected macrophages, indicating that intracellular D29 replication may occur. Much titer reduction, however, occurred prior to D29 infecting TB, attributed to the acidic macrophage environment [41]. Basra [42] studied the stability of D29 at different temperatures and pH. Approximately 2 $\log_{10}$(pfu/mL) titer reduction was observed at pH 5 after 1 h [42], which supports the hypothesis that the acidic environment in the macrophage can decrease the phage titer, although other digestive mechanisms occurring in the macrophage could also have led to the titer reduction. To counter this titer reduction and increase the chances that active phage infects TB within the macrophages, Xiong *et al.* [41] suggested repeated phage administration regimes. Other alternatives may involve encapsulation of phage and buffer in liposomes, which release these contents in the macrophage, or dry powder encapsulation of phage and buffer nanoparticles.

Prophylactic administration of D29 has also been proposed [8]. Were D29 to line the alveoli just prior to TB infection, it would have the opportunity to infect TB before macrophage uptake. The D29 progeny released upon lysis of the TB in the alveoli would offer further protection against additional TB entering the alveoli soon after. Alternatively, therapeutic treatment of TB after granuloma formation would likely require additional vectors.

For infections generating biofilms, phage therapy may require additional interventions. Darch *et al.* [43] showed that the use of a two-phage cocktail, which lysed planktonic *Pseudomonas aeruginosa* culture, did not remove all biofilm aggregates in synthetic sputum. On the other hand, some lytic phage can naturally penetrate biofilms by expressing depolymerases, which can also be applied exogenously [44, 45]. Screening for host susceptibility and depolymerase effectiveness using a bank of phage may be required [45, 46]. Phage can also be engineered to release biofilm-degrading substances upon cell lysis [46]. Additionally, D-amino acids can degrade certain biofilms [47] and have been spray dried in phage formulations with acceptable processing titer reduction [13].

Animal studies to demonstrate the feasibility of treating specific lung infections using phage should be performed prior to aerosol phage therapy in humans. When designing animal studies, it is important to consider differences in extrathoracic deposition with particle size between animals and humans; for example, much smaller particles are required to bypass the extrathoracic region and reach the lungs of mice than of humans [39, 48]. An additional factor to consider when determining the dose to nebulize is the loss of active phage due to aerosol deposition within the delivery interface. For example, aerosol deposition within a nose-only inhalation device has been shown to be substantial [48], and deposition occurs within the chamber and upon the exterior of animals in a whole-body aerosol exposure system. The use of a delivery interface optimized for use with a vibrating mesh nebulizer could result in a higher titer being inhaled by the animal than were a jet nebulizer used, thus improving the chance of successful treatment outcomes.

CONCLUSION

Pulmonary delivery of phage formulations at high titers requires a prudent choice of inhalation device. Based on data presented here, the vibrating mesh nebulizer is the recommended choice for delivering anti-TB phage D29 in animal studies, as there was a high active phage delivery rate with only a small reduction in titer due to aerosolization. In contrast, the jet nebulizer does not appear to be a good choice for D29 phage therapy because of substantial titer reduction, likely caused by stress associated with droplet production and

renebulization processes. The soft mist inhaler can deliver phage D29 at high titers quickly and conveniently and, being pocket-sized, may prove useful for self-administered phage therapy applications. Titer reduction is inhalation device- and phage strain-dependent; thus, the survival of individual phage strains within a cocktail should be tested with different delivery devices while developing phage cocktail – inhalation device combinations.

ACKNOWLEDGMENTS AND DISCLOSURES

NC gratefully thanks the Natural Sciences and Engineering Research Council of Canada, Alberta Innovates, and the University of Alberta for scholarship funding. This includes a Michael Smith Foreign Study Supplement and an Education Abroad Individual Award allowing him to perform research in Sydney, Australia. The authors thank Arlene Oatway for help with the transmission electron micrograph and Jim Fink for providing Aerogen nebulizers and equipment. This work was financially supported in part by the Australian Research Council (Discovery Project DP150103953).

APPENDIX

Appendix Notation

$C_{d,p,i}$	mass concentration of solute in the solvent droplets both exiting the mouthpiece and returning to the reservoir in the i^{th} nebulization cycle, assumed to be equal
$C_{e,p,i}$	mass concentration of solute in the solvent droplets exiting the mouthpiece in the i^{th} nebulization cycle
$C_{n,p,i}$	mass concentration of solute in the solvent exiting the nozzle in the i^{th} nebulization cycle
C_p	mass concentration of solute in the solvent
$C_{p,0}$	mass concentration of solute in the solvent initially input to the reservoir
$C_{r,p,i}$	mass concentration of solute in the solvent droplets returning to the reservoir in the i^{th} nebulization cycle
$Cu(f_{e,i})$	fraction of the initial number of phage input to the jet nebulizer which have cumulatively exited the mouthpiece over i nebulization cycles
$Cu(i^*X_i)$	average number of nebulization cycles phage which exited the mouthpiece underwent
$f_{e,i}$	fraction of the number of phage initially input to the reservoir, which exit the mouthpiece in the i^{th} nebulization cycle
i	nebulization cycle count
j	a summation index for i in $Cu(f_{e,i})$
k	a summation index for i in X_i
L	a summation index for i in $Cu(i^*X_i)$
$\dot{m}_{e,s}$	mass flow rate of solvent in droplets exiting the mouthpiece
$\dot{m}_{h,s}$	mass flow rate of solvent exiting due to humidification of air supplied by the compressor
$\dot{m}_{n,s}$	mass flow rate of solvent exiting the nozzle
$\dot{m}_p$	mass flow rate of solute
$\dot{m}_{r,s}$	mass flow rate of solvent returning to the reservoir
$\dot{m}_s$	mass flow rate of solvent
m_{1p}	mass of a single phage
$\mathcal{N}$	total number of nebulization cycles to complete aerosolization
$n_{e,p,i}$	number of phage, either active or inactive, exiting the mouthpiece in the i^{th} nebulization cycle
$n_{p,0}$	number of phage initially input to the reservoir
ρ_s	mass density of the solvent
$Q_{e,s}$	volumetric flow rate of solvent in droplets exiting the mouthpiece
$Q_{h,s}$	volumetric flow rate of solvent exiting due to humidification of air supplied by the compressor
$Q_{n,s}$	volumetric flow rate of solvent exiting the nozzle
$Q_{r,s}$	volumetric flow rate of solvent returning to the reservoir
Q_s	volumetric flow rate of solvent
t_i	time to complete the i^{th} nebulization cycle
$V_{e,s,i}$	volume of solvent in droplets exiting the mouthpiece in the i^{th} nebulization cycle
V_F	volume of solvent initially input to the reservoir, termed fill volume
$V_{h,s,i}$	equivalent liquid volume of solvent exiting the device due to humidification of air supplied by the compressor in the i^{th} nebulization cycle
$V_{n,s,i}$	volume of solvent exiting the nozzle in the i^{th} nebulization cycle
$V_{r,s,i}$	volume of solvent returning to the reservoir in the i^{th} nebulization cycle
X_i	fraction of the cumulative number of phage which have exited the mouthpiece after aerosolization is complete, which exited the mouthpiece in the i^{th} nebulization cycle

Nebulization Cycle Count Mathematical Model

A mathematical model was developed to estimate the average number of times that phage exited the nozzle and impacted the primary baffle of the jet nebulizer prior to exiting the mouthpiece.

The solvent, water in this study, can follow three paths after exiting the nozzle: 1) humidify the air supplied by the compressor and exit the nebulizer as vapor; 2) exit the mouthpiece as aerosol droplets; 3) impact the interior of the device and

return (drip back) to the reservoir. By assuming no mixing between the reservoir fluid and returning fluid in the same nebulization cycle, conservation of mass for the solvent gives

$$\dot{m}_{n,s} = \dot{m}_{h,s} + \dot{m}_{e,s} + \dot{m}_{r,s} \tag{1}$$

where $\dot{m}_{n,s}$ is the mass flow rate of the solvent exiting the nozzle, $\dot{m}_{h,s}$ is the mass flow rate of solvent which will exit the device via humidification of the air supplied by the compressor, $\dot{m}_{e,s}$ is the mass flow rate of solvent which will exit the mouthpiece of the device as aerosol droplets, and $\dot{m}_{r,s}$ is the mass flow rate of solvent which will return to the reservoir to exit the nozzle in the next nebulization cycle.

The solvent mass flow rate is related to volumetric flow rate by

$$\dot{m}_s = \rho_s {}^* Q_s \tag{2}$$

For water, ρ_s can be considered constant during jet nebulization. Eq. (1) can thus be rewritten in terms of flow rates:

$$Q_{n,s} = Q_{h,s} + Q_{e,s} + Q_{r,s} \tag{3}$$

The flow rate exiting the nozzle, $Q_{n,s}$, was determined experimentally using Tryptophan tracer assay, to be 17.64 mL/min. The flow rate exiting the mouthpiece of the device, $Q_{e,s}$, was determined to be 0.12 mL/min from the mass captured on the filter during phage experiments. The flow rate lost to humidification, $Q_{h,s}$, was calculated as the difference in flow rate determined based on mass loss from the nebulizer and mass captured on the outlet filter during phage experiments, and found to be 0.06 mL/min. This matched the theoretical amount of water required to fully humidify the air supplied by the compressor. The flow rate returning to the reservoir, $Q_{r,s}$, was thus calculated using Eq. (3), to be 17.46 mL/min.

It is assumed that solute does not exit the inhaler via humidification losses. Mass conservation for the solute (phage) is then given by

$$\dot{m}_{n,p} = \dot{m}_{e,p} + \dot{m}_{r,p} \tag{4}$$

The solute concentration in the solvent, C_p, is related to the mass flow rate by

$$\dot{m}_p = C_p {}^* Q_s \tag{5}$$

Assuming the solute remains in the droplets and reservoir fluid, Eqs. (4) and (5) can be combined to give

$$C_{n,p,i} {}^* Q_{n,s} = C_{e,p,i} {}^* Q_{e,s} + C_{r,p,i} {}^* Q_{r,s} \tag{6}$$

It is assumed that the humidification of the air supplied by the compressor occurs by evaporation of the droplets exiting the nozzle, which have a high air-liquid surface area to volume ratio, rather than from the liquid in the reservoir. The humidification due to evaporation of the primary and secondary droplets increases the solute concentration in the droplets. Let us assume that the increase in concentration in the droplets that exit the mouthpiece and that return to the reservoir is equal. Then, we can define the droplet concentration, $C_{d,p}$, as

$$C_{d,p,i} \equiv C_{e,p,i} = C_{r,p,i} \tag{7}$$

With each nebulization cycle, i, the concentration of the solute in the reservoir will increase. The concentration of solute in the reservoir in a specific cycle, i, is the same as the concentration of solute in the droplets in the previous cycle, $i-1$, as we have assumed no mixing between the reservoir fluid and returning fluid in the same cycle:

$$C_{n,p,i} = C_{r,p,i-1} = C_{d,p,i-1} \tag{8}$$

Let us define

$$C_{n,p,1} = C_{p,0} \tag{9}$$

where $C_{p,0}$ is the input mass concentration of solute in solvent. Here, $C_{n,p,1}$ represents the concentration of solute in solvent exiting the nozzle during the first nebulization cycle, when $i = 1$.

By combining Eqs. (6) and (7), and assuming that the respective volumetric flow rates are independent of nebulization cycle,

$$C_{n,p,i} {}^* Q_{n,s} = C_{d,p,i} {}^* \left(Q_{e,s} + Q_{r,s} \right) \tag{10}$$

Combining Eqs. (8) and (10)

$$C_{d,p,i-1} {}^* Q_{n,s} = C_{d,p,i} {}^* \left(Q_{e,s} + Q_{r,s} \right) \tag{11}$$

and rearranging Eq. (11) gives

$$\frac{C_{d,p,i}}{C_{d,p,i-1}} = \frac{Q_{n,s}}{\left(Q_{e,s} + Q_{r,s} \right)} \tag{12}$$

The value of $\frac{Q_{n,s}}{\left(Q_{e,s} + Q_{r,s} \right)}$ is a constant, equal to 1.0034 in the present study. This value quantifies the increase in concentration of solute in the droplets emitted from the nozzle with each nebulization cycle, due to loss of solvent associated with humidification of the air supplied by the compressor.

When $i = 1$, using Eqs. (8), (9), and (11), one finds that

$$C_{d,p,1} = \frac{Q_{n,s}}{\left(Q_{e,s} + Q_{r,s} \right)} C_{p,0} \tag{13}$$

For $i = 2$, Eq. (12) gives

$$C_{d,p,2} = \frac{Q_{n,s}}{\left(Q_{e,s} + Q_{r,s}\right)} C_{d,p,1} \tag{14}$$

Combining Eqs. (13) and (14), one finds that

$$C_{d,p,2} = \left(\frac{Q_{n,s}}{Q_{e,s} + Q_{r,s}}\right)^2 C_{p,0} \tag{15}$$

One can continue to show that in general

$$C_{d,p,i} = \left(\frac{Q_{n,s}}{Q_{e,s} + Q_{r,s}}\right)^i C_{p,0} \tag{16}$$

This equation demonstrates how the solute concentration in the droplets of a specific nebulization cycle, i, is related to the initial solute concentration in the reservoir.

In order to estimate the number of phage exiting the mouthpiece in a specific nebulization cycle, volumes are evaluated for each nebulization cycle. The volume returned to the nebulizer, $V_{r,s}$, in a specific cycle is equal to the volume exiting the nozzle, $V_{n,s}$, in the following cycle:

$$V_{n,s,i} = V_{r,s,i-1} \tag{17}$$

Eq. (17) is valid for $i = 2 \rightarrow \mathcal{N}$. For $i = 1$, the volume exiting the nozzle is assumed to be equal to the fill volume, V_F:

$$V_{n,s,1} = V_F \tag{18}$$

The time for a nebulization cycle to complete, t_i, is specified by

$$t_i = \frac{V_{n,s,i}}{Q_{n,s}} \tag{19}$$

The following volumes can then be obtained using t_i and the known flow rates:

$$V_{h,s,i} = Q_{h,s}{}^* t_i \tag{20}$$

$$V_{e,s,i} = Q_{e,s}{}^* t_i \tag{21}$$

$$V_{r,s,i} = Q_{r,s}{}^* t_i \tag{22}$$

where $V_{h,s,i}$ is the equivalent liquid volume exiting the device due to humification in a specific nebulization cycle, $V_{e,s,i}$ is the volume exiting the mouthpiece of the device as droplets in a specific nebulization cycle, and $V_{r,s,i}$ is the volume returned to the reservoir in a specific nebulization cycle.

The number of phage, either active or inactive, exiting the mouthpiece in a specific nebulization cycle, $n_{e,p,i}$, can be found according to

$$n_{e,p,i} = \frac{C_{d,p,i}{}^* V_{e,s,i}}{m_{1p}} \tag{23}$$

where m_{1p} is the mass of a single phage.

Similarly, the number of phage initially in the reservoir is

$$n_{p,0} = \frac{C_{p,0}{}^* V_F}{m_{1p}} \tag{24}$$

The fraction of the number of phage initially input to the reservoir that has exited the mouthpiece in a specific nebulization cycle, $f_{e,i}$, can therefore be found using Eqs. (16), (23), and (24), as

$$f_{e,i} = \frac{n_{e,p,i}}{n_{p,0}} = \left(\frac{Q_{n,s}}{Q_{e,s} + Q_{r,s}}\right)^{i*} \frac{V_{e,s,i}}{V_F} \tag{25}$$

The fraction of the number of phage initially input to the reservoir that have cumulatively exited the mouthpiece of the device over i nebulization cycles, $Cu(f_{e,i})$, is given by

$$Cu\left(f_{e,i}\right) = \sum_{j=1}^{j=i} f_{e,j} \tag{26}$$

where j is a summation index. To solve Eq. (26), for example, when $i = 3$,

$$\begin{aligned} Cu\left(f_{e,3}\right) &= \sum_{j=1}^{j=3} f_{e,j} = f_{e,1} + f_{e,2} + f_{e,3} \\ &= \left(\frac{Q_{n,s}}{Q_{e,s} + Q_{r,s}}\right)^{1*} \frac{V_{e,s,1}}{V_F} + \left(\frac{Q_{n,s}}{Q_{e,s} + Q_{r,s}}\right)^{2*} \frac{V_{e,s,2}}{V_F} \\ &\quad + \left(\frac{Q_{n,s}}{Q_{e,s} + Q_{r,s}}\right)^{3*} \frac{V_{e,s,3}}{V_F} \end{aligned} \tag{27}$$

The curve in Figure 4 represents the solution to Eq. (26) for every i from $i = 1$ to $i = \mathcal{N}$, where $\mathcal{N}$ represents the number of nebulization cycles when $V_{r,s,i}$ is equal to the residual volume of the nebulizer after aerosolization is complete, which was experimentally determined to be 0.5 mL during phage measurements in this study. The fraction was converted to a percentage in the plot.

Also given in Figure 4 is the average number of nebulization cycles phage that exited the mouthpiece underwent. To determine this value, one must consider that some phage are left in the residual volume of the nebulizer after aerosolization is complete.

The fraction of the cumulative number of phage that have exited the mouthpiece after $\mathcal{N}$ nebulization cycles, that exited

the mouthpiece in the specific nebulization cycle i, is termed X_i, and is given by:

$$X_i = \frac{n_{e,p,i}}{\sum_{k=1}^{k=N} n_{e,p,k}} = \frac{n_{e,p,i}}{n_{e,p,1} + n_{e,p,2} + \ldots + n_{e,p,N}} \quad (28)$$

where k is a summation index.

It can be shown that the average number of nebulization cycles phage underwent prior to exiting the mouthpiece of the jet nebulizer, $Cu(i^*X_i)$, is given by

$$Cu(i^*X_i) = \sum_{L=1}^{L=N} (L^*X_L) = (1^*X_1) + (2^*X_2) + \ldots + (N^*X_N) \quad (29)$$

where L is a summation index.

The average number of nebulization cycles the phage underwent prior to exiting the mouthpiece of the jet nebulizer was thus determined to be 96 in the present study, with the final phage exiting the mouthpiece having undergone N=269 nebulization cycles. Assuming that every time a phage exits the nozzle it impacts the primary baffle, the nebulization cycle count i corresponds to the number of baffle impactions the phage underwent.

Other parameters such as total nebulization time and total volumes lost to humidification and exiting the mouthpiece can also be obtained using summations from 1 to N.

REFERENCES

1. Ventola CL. The antibiotic resistance crisis. Part 1: causes and threats. PT. 2015;40(4):277–83.
2. World Health Organization. Multidrug-resistant tuberculosis (MDR-TB): 2016 Update. 2016 Available from: http://www.who.int/tb/challenges/mdr/mdr_tb_factsheet.pdf . Accessed 21 Feb 2017.
3. Udwadia ZF, Amale RA, Ajbani KK, Rodrigues C. Totally drug-resistant tuberculosis in India. Clin Infect Dis. 2012;54(4):579–81.
4. World Health Organization. Drug-resistant TB: Totally drug-resistant TB FAQ. 2017 Available from: http://www.who.int/tb/areas-of-work/drug-resistant-tb/totally-drug-resistant-tb-faq/en/. Accessed 21 Feb 2017.
5. Abedon ST, Kuhl SJ, Blasdel BG, Kutter EM. Phage treatment of human infections. Bacteriophage. 2011;1(2):66–85.
6. Kutateladze M, Adamia R. Bacteriophages as potential new therapeutics to replace or supplement antibiotics. Trends Biotechnol. 2010;28(12):591–5.
7. Verbeken G, Huys I, Pirnay J-P, Jennes S, Chanishvili N, Scheres J, *et al.* Taking bacteriophage therapy seriously: a moral argument. Biomed Res Int. 2014;2014:621316.
8. Hatfull GF, Vehring R. Respirable bacteriophage aerosols for the prevention and treatment of tuberculosis. In: Hickey AJ, Misra A, Fourie PB, editors. Drug delivery systems for tuberculosis prevention and treatment. Chichester: John Wiley & Sons, Ltd.; 2016. p. 277–92.
9. Loc-Carrillo C, Abedon ST. Pros and cons of phage therapy. Bacteriophage. 2011;1(2):111–4.
10. Kutter E, Sulakvelidze A. Bacteriophages: biology and applications. Boca Raton: CRC Press; 2005.
11. Hoe S, Semler DD, Goudie AD, Lynch KH, Matinkhoo S, Finlay WH, *et al.* Respirable bacteriophages for the treatment of bacterial lung infections. J Aerosol Med Pulm Drug Deliv. 2013;26(6):317–35.
12. Kutter E, de Vos D, Gvasalia G, Alavidze Z, Gogokhia L, Kuhl S, *et al.* Phage therapy in clinical practice: treatment of human infections. Curr Pharm Biotechnol. 2010;11(1):69–86.
13. Hoe S, Boraey MA, Ivey JW, Finlay WH, Vehring R. Manufacturing and device options for the delivery of biotherapeutics. J Aerosol Med Pulm Drug Deliv. 2014;27(5):315–28.
14. Golshahi L, Seed KD, Dennis JJ, Finlay WH. Toward modern inhalational bacteriophage therapy: nebulization of bacteriophages of Burkholderia cepacia complex. J Aerosol Med Pulm Drug Deliv. 2008;21(4):351–60.
15. Matinkhoo S, Lynch KH, Dennis JJ, Finlay WH, Vehring R. Spray-dried respirable powders containing bacteriophages for the treatment of pulmonary infections. J Pharm Sci. 2011;100(12):5197–205.
16. Leung SY, Parumasivam T, Gao FG, Carrigy NB, Vehring R, Finlay WH, *et al.* Production of inhalation phage powders using spray freeze drying and spray drying techniques for treatment of respiratory infections. Pharm Res. 2016;33(6):1486–96.
17. Golshahi L, Lynch KH, Dennis JJ, Finlay WH. *In vitro* lung delivery of bacteriophages KS4-M and ϕKZ using dry powder inhalers for treatment of Burkholderia cepacia complex and Pseudomonas Aeruginosa infections in cystic fibrosis. J Appl Microbiol. 2011;110(1):106–17.
18. Parracho HMRT, Burrowes BH, Enright MC, McConville ML, Harper DR. The role of regulated clinical trials in the development of bacteriophage therapeutics. J Mol Genet Med. 2012;6:279–86.
19. Verbeken G, Pirnay J-P, de Vos D, Jennes S, Zizi M, Lavigne R, *et al.* Optimizing the European regulatory framework for sustainable bacteriophage therapy in human medicine. Arch Immunol Ther Exp. 2012;60(3):161–72.
20. Abedon ST. Phage therapy of pulmonary infections. Bacteriophage. 2015;5(1):1–13.
21. Semler DD, Goudie AD, Finlay WH, Dennis JJ. Aerosol phage therapy efficacy in Burkholderia cepacia complex respiratory infections. Antimicrob Agents Chemother. 2014;58(7):4005–13.
22. Liu K-Y, Yang W-H, Dong X-K, Cong L-M, Li N, Li Y, *et al.* Inhalation study of mycobacteriophage D29 aerosol for mice by endotracheal route and nose-only exposure. J Aerosol Med Pulm Drug Deliv. 2016;29(5):393–405.
23. Cooper CJ, Denyer SP, Maillard J-Y. Stability and purity of a bacteriophage cocktail preparation for nebulizer delivery. Lett Appl Microbiol. 2013;58(2):118–22.
24. Sahota JS, Smith CM, Radhakrishnan P, Winstanley C, Goderdzishvili M, Chanishvili N, *et al.* Bacteriophage delivery by nebulization and efficacy against phenotypically diverse Pseudomonas Aeruginosa from cystic fibrosis patients. J Aerosol Med Pulm Drug Deliv. 2015;28(5):353–60.
25. Froman S, Will DW, Bogen E. Bacteriophage active against virulent mycobacterium tuberculosis I. Isolation and activity. Am J Public Health Nations Health. 1954;44(10):1326–33.
26. phagesDB.org. Phage hunting procedure & protocols. 2016 December 2. Available from: phagesdb.org/workflow/.
27. Engel M, Heinrichs S. Use of tiotropium salts in the treatment of moderate persistent asthma. 2015. Patent US 20150224090 A1.
28. Dalby R, Spallek M, Voshaar T. A review of the development of Respimat soft mist inhaler. Int J Pharm. 2004;283(1–2):1–9.

29. Dalby R, Eicher J, Zierenberg B. Development of Respimat® Soft Mist™ Inhaler and its clinical utility in respiratory disorders. Med Devices (Auckl). 2011;4:145–55.
30. Finlay WH. The mechanics of inhaled pharmaceutical aerosols: an introduction. San Diego: Academic Press; 2001.
31. Fink JB. New technology offers new opportunities: continuous bronchodilator therapy during mechanical ventilation. Available from: https://www.aerogen.com/uploads/Publications/Continuous%20Bronchodilator%20Therapy%20During%20Mechanical%20Ventilation%20Jim%20Fink.pdf. Accessed 22 Feb 2017.
32. May KR. The collison nebulizer: description, performance and application. J Aerosol Sci. 1973;4(3):235–43.
33. Lentz YK, Worden LR, Anchordoquy TJ, Lengsfeld CS. Effect of jet nebulization on DNA: identifying the dominant degradation mechanism and mitigation methods. J Aerosol Sci. 2005;36(8):973–90.
34. Liu K, Wen Z, Yang W, Wang J, Hu L, Dong X, *et al.* Impact of relative humidity and collection media on mycobacteriophage D29 aerosol. Appl Environ Microbiol. 2012;78(5):1466–72.
35. Arulmuthu ER, Williams DJ, Baldascini H, Versteeg HK, Hoare M. Studies on aerosol delivery of plasmid DNA using a mesh nebulizer. Biotechnol Bioeng. 2007;98(5):939–55.
36. Sidler-Moix A-L, Di Paolo ER, Dolci U, Berger-Gryllaki M, Cotting J, Pannatier A. Physicochemical aspects and efficiency of albuterol nebulization: comparison of three aerosol types in an *in vitro* pediatric model. Respir Care. 2015;60(1):38–46.
37. Fédération Antadir Commission Medico-Technique & Sociale. Fiche de synthese du dispositif: Pari Boy SX / Pari LC® Sprint SP. 2007 Available from: http://www.antadir.com/uploads/product/95/pdf/synthese-pari-lc-sprint-v4-inter.pdf. Accessed 12 May 2017.
38. Wachtel H, Ziegler J. Improved assessment of inhaler device performance using laser diffraction. Respiratory Drug Deliv VIII. 2002;2:379–81.
39. Carrigy NB, Martin AR, Finlay WH. Use of extrathoracic deposition models for patient-specific dose estimation during inhaler design. Curr Pharm Des. 2015;21(27):3984–92.
40. Vandal OH, Nathan CF, Ehrt S. Acid resistance in mycobacterium tuberculosis. J Bacteriol. 2009;191(15):4714–21.
41. Xiong X, Zhang HM, Wu TT, Xu L, Gan YL, Jiang LS, *et al.* Titer dynamic analysis of D29 within MTB-infected macrophages and effect on immune function of macrophages. Exp Lung Res. 2014;40(2):86–98.
42. Basra SK. The isolation and characterization of phages with lytic activity against Mycobacterium avium subspecies paratuberculosis, and their application using Bioluminescent assay in real-time Loop-mediated isothermal amplification assay for rapid detection. Master of Science Thesis. Department of Food Science, University of Guelph. 2013. Guelph, ON, Canada.
43. Darch SE, Kragh KN, Abbott EA, Bjarnsholt T, Bull JJ, Whiteley M. Phage inhibiting pathogen dissemination by targeting bacterial migrants in a chronic infected model. mBio. 2017;8(2):e00240–17.
44. Abedon ST. Bacteriophages and biofilms: ecology, phage therapy, plaques. New York: Nova Science Publishers, Inc.; 2011.
45. Drulis-Kawa Z, Majkowska-Skrobek G, Maciejewska B, Delattre A-S, Lavigne R. Learning from bacteriophages – advantages and limitations of phage and phage-encoded protein applications. Curr Protein Pept Sci. 2012;13(8):699–722.
46. Lu TK, Collins JJ. Dispersing biofilms with engineered enzymatic bacteriophage. PNAS. 2007;104(27):11197–202.
47. Kolodkin-Gal I, Romero D, Cao S, Clardy J, Kolter R, Losick R. D-amino acids trigger biofilm disassembly. Science. 2010;328(5978):627–9.
48. Nadithe V, Rahamatalla M, Finlay WH, Mercer JR, Samuel J. Evaluation of nose-only aerosol inhalation chamber and comparison of experimental results with mathematical simulation of aerosol deposition in mouse lungs. J Pharm Sci. 2003;92(5):1066–76.